Ab initio calculations of transition amplitudes and hyperfine *A* and *B* constants of Ga III

Narendra Nath Dutta,[1] Sourav Roy,[1] Gopal Dixit,[2] and Sonjoy Majumder[1]
[1]*Department of Physics and Meteorology, Indian Institute of Technology-Kharagpur, Kharagpur-721302, India*
[2]*Centre for Free-Electron Laser Science, DESY, Notkestrasse 85, D-22607 Hamburg, Germany*
(Received 19 September 2012; published 2 January 2013)

In this paper, the $E1$, $E2$, and $M1$ transition amplitudes are calculated along with the hyperfine A and B constants of doubly ionized gallium using the relativistic coupled-cluster approach. Electron correlations and the Gaunt interactions are considered to all orders using the coupled-cluster theory in a relativistic framework and their contributions are discussed explicitly in the calculations of all these amplitudes. Some interesting features of the correlation effects on the Gaunt interactions are noticed in the calculations of the hyperfine constants. The lifetimes of some low-lying states are also calculated using the transition amplitudes obtained by the present theory and the experimental transition energies. The calculated $E1$ transition amplitudes and lifetimes are in good agreement with the results obtained by the other theories and experiment. The hyperfine splitting of the ground states of ^{71}Ga III and ^{69}Ga III are found to be about 35 and 27.5 GHz, respectively, which shows the importance of these isotopes for the possible use of microwave frequency standards. The calculated hyperfine constants are associated with linewidth estimations of some transition lines in the visible and ultraviolet regions of electromagnetic spectrum.

DOI: 10.1103/PhysRevA.87.012501 PACS number(s): 32.10.−f, 31.15.bw, 95.30.Ky

I. INTRODUCTION

Like the trapping of singly ionized atoms, the trapping of multiply ionized atoms is the subject of recent research interest in physics due to their competence as candidates of fundamental constants and due to their use for frequency standards in the microwave region. Trapped Yb III has been proposed already as a good candidate to use for a most sensitive test of time variation of the fine-structure constant [1,2]. Similarly, trapped ^{229}Th IV has been considered to have the potential to be used as a nuclear clock [1,3]. So it is natural to investigate some other multiply ionized atoms to propose them in this category for their use in such applications. Our investigation on the ground-state hyperfine splitting of the two stable isotopes of doubly ionized gallium is important from this point of view.

Improvement of high-resolution spectrographs in space telescopes demands accurate data to explore abundances of different atomic species in different astronomical systems. Recently, evidence of the presence of Ga III has been reported in the ultraviolet spectra of the subdwarf B (sdB) stars, subdwarf OB (sdOB) stars, magnetic Si stars, He-weak stars, hot HgMn stars, and several other astronomical systems [4–7]. However, very few theoretical calculations associated with the allowed transition, i.e., $E1$ transition, lines of this element are available in the literature [8–11]. This ion is also important as an impurity concentration indicator in hot plasmas [8]. So the different forbidden transition, i.e., $E2$ and $M1$ transition, lines of this ion may play a crucial role in the plasma modeling. The hyperfine-structure calculations of this ion are most likely associated with the difference of Ga abundance estimations in between the visible and ultraviolet spectra of the HgMn stars [6]. This particular phenomena was named "The Gallium Problem" by Dworetsky *et al.* [6]. The hyperfine calculations are also very important to determine the isotopic abundances in the different astronomical systems.

In the last three decades, in a number of approaches, theoretical calculations have been carried out to determine the oscillator strengths (f) of $E1$ transitions between very few low-lying states of Ga III as a member of the Cu isoelectronic sequence [8,9,11]. Curtis and Theodosiou [8] calculated the lifetimes of a few low-lying states and the f values between them using the Coulomb approximated Hartree-Slater core potential approach. Migdalek and Baylis [9] studied the core polarization effects by including it in a relativistic Hartree-Fock method as well as in a relativistic semiempirical model potential approach to calculate the f values. The quantum defect theory was used by Owono Owono *et al.* [11] to produce the transition matrix elements of the electric dipole operator in the calculations of the corresponding strengths. Relativistic third-order many-body perturbation theory was applied by Chou and Johnson [10] to find the $E1$ transition amplitudes of the principal transitions of this element. The lifetimes of a few low-lying states of this element were measured experimentally by the beam-foil technique using a field-emission ion source [12]. However, from a theoretical point of view, there are no detailed discussions on the trends of the correlation and relativistic effects in these calculations. Moreover, atomic data for the forbidden transition lines of this element are not present in the literature to the best of our knowledge.

Here, we have performed *ab initio* calculations of transition amplitudes of the $E1$, $E2$, and $M1$ transitions between a few low-lying states of Ga III using nonlinear coupled-cluster theory with single, double, and partial triple excitations in a relativistic framework. Both the hyperfine A and B constants are determined for a few states of this ion with mass number 71 and 69, which are the only two stable isotopes of Ga [13]. The lifetimes of a few low-lying states are calculated using these transition amplitudes and are compared with the other theoretical and experimental results. As an improvement of the atomic Hamiltonian, the Gaunt interaction [14], which is the unretarded part of the Breit interaction, has been implemented self-consistently [15]. The retardation part of the Breit interaction contributes little compared to the Gaunt part and hence is neglected in our calculations [16]. The results are presented at the Dirac-Fock and coupled-cluster levels of calculations along with the correlation and Gaunt contributions. The trends of the correlation effects on the Gaunt contributions in the calculations of the hyperfine constants are analyzed graphically.

II. THEORY

According to the coupled-cluster (CC) theory, a single valence atomic state wave function $|\Psi_v\rangle$ associated with a valence electron in the vth orbital can be expressed in terms of the closed-shell cluster operator T, the open-shell cluster operator S_v, and the corresponding reference state wave function $|\Phi_v\rangle$ as follows [17–20]:

$$|\Psi_v\rangle = e^T\{1 + S_v\}|\Phi_v\rangle. \tag{2.1}$$

The reference state $|\Phi_v\rangle$ is generated at the Dirac-Fock (DF) level for V^{N-1} potential, where N is the total number of electrons of the atomic system [15,21]. The energy eigenvalue equation of this atomic system is given by

$$H|\Psi_v\rangle = E|\Psi_v\rangle, \tag{2.2}$$

where H is the atomic Hamiltonian which can be written including the Gaunt interaction with the Coulomb interaction as [15]

$$H = \sum_{i=1}^{N}\Bigg[c\overrightarrow{\alpha_i}\cdot\overrightarrow{p_i} + (\beta_i - 1)c^2 + V_{\rm nuc}(r_i) + \sum_{j>i}^{N}\left(\frac{1}{r_{ij}} - \frac{\overrightarrow{\alpha_i}\cdot\overrightarrow{\alpha_j}}{r_{ij}}\right)\Bigg]. \tag{2.3}$$

Solutions of these energy eigenvalue equations corresponding to two different valence orbitals can be applied to generate the general matrix element of an operator $\hat{O}$. This general matrix element can be written by using the CC theory as

$$O_{fi} = \frac{\langle\Psi_f|\hat{O}|\Psi_i\rangle}{\sqrt{\langle\Psi_f|\Psi_f\rangle\langle\Psi_i|\Psi_i\rangle}} = \frac{\langle\Phi_f|\{1 + S_f^\dagger\}e^{T^\dagger}\hat{O}e^T\{1 + S_i\}|\Phi_i\rangle}{\sqrt{\langle\Phi_f|\{1 + S_f^\dagger\}e^{T^\dagger}e^T\{1 + S_f\}|\Phi_f\rangle\langle\Phi_i|\{1 + S_i^\dagger\}e^{T^\dagger}e^T\{1 + S_i\}|\Phi_i\rangle}} \tag{2.4}$$

To evaluate this general matrix element, one needs the knowledge of single particle reduced matrix elements of the corresponding operator [18]. For the $E1$ (in length gauge), $E2$ (in length gauge), and $M1$ transition operators, these are as follows [22,23]:

$$\langle\kappa_i||e1||\kappa_j\rangle = \frac{3}{k}\langle\kappa_i||C^{(1)}||\kappa_j\rangle\int_0^\infty dr\Bigg(j_1(kr)[P_i(r)P_j(r) + Q_i(r)Q_j(r)] + j_2(kr)\left\{\frac{\kappa_i - \kappa_j}{2}[P_i(r)Q_j(r) + Q_i(r)P_j(r)] + [P_i(r)Q_j(r) - Q_i(r)P_j(r)]\right\}\Bigg), \tag{2.5}$$

$$\langle\kappa_i||e2||\kappa_j\rangle = \frac{15}{k^2}\langle\kappa_i||C^{(2)}||\kappa_j\rangle\int_0^\infty dr\Bigg(j_2(kr)[P_i(r)P_j(r) + Q_i(r)Q_j(r)] + j_3(kr)\left\{\frac{\kappa_i - \kappa_j}{3}[P_i(r)Q_j(r) + Q_i(r)P_j(r)] + [P_i(r)Q_j(r) - Q_i(r)P_j(r)]\right\}\Bigg), \tag{2.6}$$

and

$$\langle\kappa_i||m1||\kappa_j\rangle = \frac{6}{\alpha k}\langle-\kappa_i||C^{(1)}||\kappa_j\rangle\int_0^\infty dr\left\{\frac{\kappa_i + \kappa_j}{2}j_1(kr)[P_i(r)Q_j(r) + Q_i(r)P_j(r)]\right\}. \tag{2.7}$$

Here, $k = \omega\alpha$, where $\omega = \epsilon_i - \epsilon_j$ is the excitation energy and α is the fine-structure constant. $j_l(kr)$ is the spherical Bessel function of order l. $\frac{P_i(r)}{r}$ and $\frac{Q_i(r)}{r}$ are the large and small components, respectively, of the radial part of the DF wave function.

The hyperfine energy of an atomic system in the presence of the magnetic dipole and electric quadrupole moments of the nucleus is written as [18,24]

$$H_{\rm hfs} = \frac{AK}{2} + \frac{1}{2}\frac{3K(K+1) - 4J(J+1)I(I+1)}{2I(2I-1)2J(2J-1)}B. \tag{2.8}$$

Here, $K = F(F+1) - I(I+1) - J(J+1)$, and A and B are the two constants associated with the magnetic dipole and electric quadrupole moments of the nucleus, respectively. Mathematically, these two constants are written as [15,24]

$$A = \mu_N g_I\frac{\langle J||\mathbf{T}^{(1)}||J\rangle}{\sqrt{J(J+1)(2J+1)}} \tag{2.9}$$

and

$$B = 2eQ\sqrt{\frac{2J(2J-1)}{(2J+1)(2J+2)(2J+3)}}\langle J||\mathbf{T}^{(2)}||J\rangle, \tag{2.10}$$

where μ_N is the nuclear magneton, g_I is the g factor, and Q is the quadrupole moment of the nucleus. The operators $\mathbf{T}^{(1)}$ and $\mathbf{T}^{(2)}$ are given explicitly in Ref. [24]. Here, we present the single particle reduced matrix elements of these operators as follows [24]:

$$\langle\kappa_i||t^{(1)}||\kappa_j\rangle = -\langle-\kappa_i||C^{(1)}||\kappa_j\rangle(\kappa_i + \kappa_j)\int_0^\infty dr\frac{1}{r^2} \times\{P_i(r)Q_j(r) + Q_i(r)P_j(r)\} \tag{2.11}$$

and

$$\langle\kappa_i||t^{(2)}||\kappa_j\rangle = -\langle\kappa_i||C^{(2)}||\kappa_j\rangle\int_0^\infty dr\frac{1}{r^3} \times\{P_i(r)P_j(r) + Q_i(r)Q_j(r)\}. \tag{2.12}$$

The reduced matrix element $\langle\kappa_i||C^{(k)}||\kappa_j\rangle$ is given in Ref. [24].

III. RESULTS AND DISCUSSIONS

The quality of the correlated wave functions generated by the relativistic coupled-cluster (RCC) method is based on the quality of the DF orbital wave functions. The DF orbitals of triply ionized Ga are generated from the universal Gaussian-type orbital (GTO) basis functions with $\alpha_0 = 0.006\,60$ and $\beta = 2.80$ for the Dirac-Coulomb Hamiltonian [21,25,26]. The DF solutions of bound orbital energies and matrix elements of the different radial operators obtained from the GRASP92 code are taken as standards to fit these universal parameters [27]. The nuclei are considered to have a Fermi-type charge distribution function [21]. The number of GTO basis functions for s, p, d, f, and g symmetries are considered as 33, 28, 21, 18, and 15, respectively, at the DF level of calculations. At the CC level, according to the convergence of the core correlation energy, the numbers of active orbitals for the abovementioned symmetries are taken as 12, 11, 10, 9, and 8, respectively [25]. The good quality of the correlated wave functions is verified by the agreement (average deviation of 3.7%) between the reduced matrix elements of the electric dipole operator in length and velocity gauge forms. The Gaunt interaction is included at both the DF and CC levels keeping all the abovementioned parameters unaltered. In the following discussions, the correlation contribution ($\Delta_{\rm corr}$) is defined by the difference between the CC and DF results for the Dirac-Coulomb Hamiltonian, whereas the Gaunt contribution ($\Delta_{\rm Gaunt}$) is defined by the difference between the CC results for the Dirac-Coulomb-Gaunt Hamiltonian and the Dirac-Coulomb Hamiltonian [15].

In Table I, the calculated length gauge values of the $E1$ transition amplitudes are presented with the correlation and Gaunt contributions. The wavelengths are quoted using the excitation energies of the National Institute of Standards and Technology (NIST) [28]. As seen from Table I, these transitions fall in the ultraviolet, visible, and near infrared regions of the electromagnetic spectrum. The transition amplitudes of the resonance transitions, i.e., $4s\,^2S_{1/2} \rightarrow 4p\,^2P_{1/2,3/2}$ transitions, are found to be about 11% correlated, which leads to about 22% correlation contributions to the corresponding oscillator strengths [26]. However, the Gaunt effects are much less significant compared to the correlations not only for these transitions but also for all the other transitions as presented in Table I. The strengths of the $4s\,^2S_{1/2} \rightarrow 5p\,^2P_{1/2,3/2}$ transitions are relatively weak, but are strongly correlated as can be seen from this table. The other $E1$ transition amplitudes having more than 10% correlation contributions are the $4p\,^2P_{1/2} \rightarrow 5d\,^2D_{3/2}$ and $4p\,^2P_{3/2} \rightarrow 5d\,^2D_{3/2,5/2}$ transitions (about 12.5%). The Gaunt contributions to all the $E1$ transitions, except the $4s\,^2S_{1/2} \rightarrow 5p\,^2P_{3/2}$ (about 0.56%) and $4p\,^2P_{3/2} \rightarrow 5d\,^2D_{3/2}$ (about 0.12%) transitions, belong to the figures of less than 0.1%.

TABLE I. Calculated $E1$ transition amplitudes with the correlation and Gaunt contributions (in a.u.). The wavelengths λ are presented in Å.

Transition	λ	DF	$\Delta_{\rm corr}$	$\Delta_{\rm Gaunt}$	Total
$4s\,^2S_{1/2} \rightarrow 4p\,^2P_{1/2}$	1534.46	1.8605	−0.2016	0.0005	1.6594
$\rightarrow 4p\,^2P_{3/2}$	1495.04	2.6332	−0.2832	0.0007	2.3507
$\rightarrow 5p\,^2P_{1/2}$	622.02	0.0464	0.0611	−0.0001	0.1074
$\rightarrow 5p\,^2P_{3/2}$	619.95	0.0375	0.0871	−0.0007	0.1239
$4p\,^2P_{1/2} \rightarrow 5s\,^2S_{1/2}$	1323.15	1.1557	−0.0253	0.0003	1.1307
$\rightarrow 4d\,^2D_{3/2}$	1267.15	3.0410	−0.2328	0.0009	2.8091
$\rightarrow 6s\,^2S_{1/2}$	817.01	0.3327	−0.0015	0.0001	0.3313
$\rightarrow 5d\,^2D_{3/2}$	806.33	0.6503	−0.0812	−0.0003	0.5688
$4p\,^2P_{3/2} \rightarrow 5s\,^2S_{1/2}$	1353.93	1.6873	−0.0367	0.0014	1.6520
$\rightarrow 4d\,^2D_{3/2}$	1295.36	1.3782	−0.1036	0.0007	1.2753
$\rightarrow 4d\,^2D_{5/2}$	1293.45	4.1303	−0.3106	0.0023	3.8220
$\rightarrow 6s\,^2S_{1/2}$	828.65	0.4782	−0.0029	0.0003	0.4756
$\rightarrow 5d\,^2D_{3/2}$	817.66	0.2848	−0.0359	−0.0003	0.2486
$\rightarrow 5d\,^2D_{5/2}$	817.24	0.8601	−0.1076	−0.0006	0.7519
$5s\,^2S_{1/2} \rightarrow 5p\,^2P_{1/2}$	4995.32	3.9667	−0.1128	0.0005	3.8544
$\rightarrow 5p\,^2P_{3/2}$	4864.39	5.5958	−0.1584	0.0004	5.4378
$4d\,^2D_{3/2} \rightarrow 5p\,^2P_{1/2}$	5995.53	3.7411	−0.0474	−0.0007	3.6930
$\rightarrow 5p\,^2P_{3/2}$	5807.90	1.6570	−0.0207	−0.0006	1.6357
$\rightarrow 4f\,^2F_{5/2}$	2418.61	6.2247	−0.2301	−0.0001	5.9945
$4d\,^2D_{5/2} \rightarrow 5p\,^2P_{3/2}$	5846.54	4.9909	−0.0625	−0.0017	4.9267
$\rightarrow 4f\,^2F_{5/2}$	2425.28	1.6677	−0.0615	0.0001	1.6063
$\rightarrow 4f\,^2F_{7/2}$	2424.90	7.4586	−0.2754	0.0001	7.1833
$5p\,^2P_{1/2} \rightarrow 6s\,^2S_{1/2}$	3731.21	2.5658	−0.0552	0.0002	2.5108
$\rightarrow 5d\,^2D_{3/2}$	3518.38	5.4298	−0.1566	0.0015	5.2747
$5p\,^2P_{3/2} \rightarrow 6s\,^2S_{1/2}$	3807.77	3.7279	−0.0781	0.0027	3.6525
$\rightarrow 5d\,^2D_{3/2}$	3586.37	2.4679	−0.0700	0.0016	2.3995
$\rightarrow 5d\,^2D_{5/2}$	3578.30	7.3860	−0.2102	0.0047	7.1805
$4f\,^2F_{5/2} \rightarrow 5d\,^2D_{3/2}$	26 630.24	7.5026	0.0093	0.0000	7.5119
$\rightarrow 5d\,^2D_{5/2}$	26 191.72	2.0016	0.0025	0.0000	2.0041
$4f\,^2F_{7/2} \rightarrow 5d\,^2D_{5/2}$	26 236.39	8.9505	0.0009	−0.0001	8.9513

TABLE II. Comparisons of $E1$ transition amplitudes obtained by the present theory and other methods (in a.u.).

Transition	Present	a	b	c	d
$4s\ ^2S_{1/2} \rightarrow 4p\ ^2P_{1/2}$	1.6594	1.6251	1.6425	1.6263	1.7240
$4s\ ^2S_{1/2} \rightarrow 4p\ ^2P_{3/2}$	2.3507	2.2366	2.3267	2.3042	2.3254
$4p\ ^2P_{1/2} \rightarrow 4d\ ^2D_{3/2}$	2.8091			2.7550	
$4p\ ^2P_{3/2} \rightarrow 4d\ ^2D_{3/2}$	1.2753			1.2505	
$4p\ ^2P_{3/2} \rightarrow 4d\ ^2D_{5/2}$	3.8220			3.7487	

[a]Reference [11]. Relativistic supersymmetry inspired quantum defect theory.
[b]Reference [10]. Relativistic many-body perturbation theory.
[c]Reference [8]. Coulomb approximation technique with a Hartree-Slater core.
[d]Reference [12]. Experimental results.

The $E1$ transition amplitudes computed by the CC theory are compared with the other theoretical calculations and experimental measurements in Table II. These theoretical calculations are based on the quantum defect theory (QDT), the relativistic many-body perturbation theory (MBPT), and the use of a Coulomb-approximated Hartree-Slater core (CAHS) [8,10,11]. Owono Owono *et al.* [11] calculated the oscillator strengths of $E1$ transitions using the relativistic supersymmetry inspired QDT where they treated the electric dipole operator as a simple radial operator r and as different radial functions proposed by Migdalek [29], Migdalek and Baylis [9], Hameed *et al.* [30], and Weisheit [31]. However, all these dipole operator forms produced the same results for Ga III. The $E1$ transition amplitudes are calculated from these oscillator strengths and the transition energies as proposed by Owono Owono *et al.* [11]. Similarly, the calculated oscillator strengths and compiled transition energies by Curtis and Theodosiou are used to calculate the amplitudes [8]. Only, direct reporting of the amplitudes are available by the third-order MBPT calculations of Chou and Johnson [10]. The experimental results are extracted from the corresponding lifetime measurements and the use of excitation energies of the NIST [12,28]. In Table II, one can find excellent agreement between the present CC results and the MBPT calculations. The present results also agree well with the theoretical values obtained by the QDT and CAHS methods as well as with the experimental measurements.

The length gauge values of the $E2$ transition amplitudes are presented in Table III with the correlation and Gaunt contributions. The wavelengths from the ultraviolet to mid-infrared regions are reported for these transition lines in the same table [28]. There are few cases in the $E1$ transitions where correlations contribute more than 10% to the amplitudes, whereas not a single such case is found to take place in the $E2$ transitions. The correlation contributions to these

TABLE III. Calculated $E2$ transition amplitudes with the correlation and Gaunt contributions (in a.u.). The wavelengths λ are presented in Å.

Transition	λ	DF	Δ_{corr}	Δ_{Gaunt}	Total
$4s\ ^2S_{1/2} \rightarrow 4d\ ^2D_{3/2}$	694.03	5.5825	−0.3512	0.0023	5.2336
$\rightarrow 4d\ ^2D_{5/2}$	693.48	6.8298	−0.4329	0.0031	6.4000
$\rightarrow 5d\ ^2D_{3/2}$	528.57	1.2003	−0.0865	−0.0001	1.1137
$\rightarrow 5d\ ^2D_{5/2}$	528.40	1.4789	−0.1099	0.0001	1.3691
$4p\ ^2P_{1/2} \rightarrow 4p\ ^2P_{3/2}$	58 199.43	6.8912	−0.3965	0.0038	6.4985
$\rightarrow 5p\ ^2P_{3/2}$	1040.20	4.5333	−0.2501	−0.0001	4.2831
$\rightarrow 4f\ ^2F_{5/2}$	831.51	8.6177	−0.5811	0.0044	8.0410
$4p\ ^2P_{3/2} \rightarrow 5p\ ^2P_{1/2}$	1065.21	4.8060	−0.2530	0.0053	4.5583
$\rightarrow 5p\ ^2P_{3/2}$	1059.13	4.7088	−0.2512	0.0032	4.4608
$\rightarrow 4f\ ^2F_{5/2}$	843.56	4.7217	−0.3115	0.0046	4.4148
$\rightarrow 4f\ ^2F_{7/2}$	843.51	11.5670	−0.7582	0.0113	10.8201
$5s\ ^2S_{1/2} \rightarrow 4d\ ^2D_{3/2}$	29 943.53	17.3600	−0.6011	0.0002	16.7591
$\rightarrow 4d\ ^2D_{5/2}$	28 956.63	21.3255	−0.7368	0.0009	20.5896
$\rightarrow 5d\ ^2D_{3/2}$	2064.37	19.7824	−0.7474	0.0096	19.0446
$\rightarrow 5d\ ^2D_{5/2}$	2061.70	24.1585	−0.9164	0.0109	23.2530
$4d\ ^2D_{3/2} \rightarrow 4d\ ^2D_{5/2}$		10.3382	−0.4274	0.0001	9.9109
$\rightarrow 6s\ ^2S_{1/2}$	2299.90	6.1806	−0.1706	−0.0032	6.0068
$\rightarrow 5d\ ^2D_{3/2}$	2217.23	10.3299	−0.2543	−0.0002	10.0754
$\rightarrow 5d\ ^2D_{5/2}$	2214.15	6.7312	−0.1662	−0.0005	6.5645
$4d\ ^2D_{5/2} \rightarrow 6s\ ^2S_{1/2}$	2305.94	7.6397	−0.2098	−0.0033	7.4266
$\rightarrow 5d\ ^2D_{3/2}$	2222.84	6.8091	−0.1669	0.0004	6.6426
$\rightarrow 5d\ ^2D_{5/2}$	2219.74	13.5555	−0.3337	0.0001	13.2219
$5p\ ^2P_{1/2} \rightarrow 5p\ ^2P_{3/2}$		31.3367	−1.0879	0.0102	30.2590
$\rightarrow 4f\ ^2F_{5/2}$	4053.99	39.3351	−1.0852	0.0038	38.2537
$5p\ ^2P_{3/2} \rightarrow 4f\ ^2F_{5/2}$	4144.53	21.1690	−0.5755	0.0058	20.5993
$\rightarrow 4f\ ^2F_{7/2}$	4143.41	51.8503	−1.4389	0.0144	50.4258
$4f\ ^2F_{5/2} \rightarrow 4f\ ^2F_{7/2}$		19.0191	−0.3333	−0.0001	18.6857
$6s\ ^2S_{1/2} \rightarrow 5d\ ^2D_{3/2}$	61 682.32	63.6698	−1.5648	0.0000	62.1050
$\rightarrow 5d\ ^2D_{5/2}$	59 379.60	78.1477	−1.9222	0.0025	76.2280
$5d\ ^2D_{3/2} \rightarrow 5d\ ^2D_{5/2}$		41.2077	−1.3390	0.0002	39.8689

TABLE IV. Calculated $M1$ transition amplitudes with the correlation and Gaunt contributions (in a.u.). The wavelengths λ are presented in Å.

Transition	λ	DF	Δ_{corr}	Δ_{Gaunt}	Total
$4p\,^2P_{1/2} \rightarrow 4p\,^2P_{3/2}$	58 199.43	1.1545	0.0002	0.0000	1.1547
$\rightarrow 5p\,^2P_{3/2}$	1040.20	0.0113	0.0005	0.0002	0.0120
$4p\,^2P_{3/2} \rightarrow 5p\,^2P_{1/2}$	1065.21	0.0116	0.0003	0.0003	0.0122
$4d\,^2D_{3/2} \rightarrow 4d\,^2D_{5/2}$		1.5491	0.0003	0.0000	1.5494
$\rightarrow 5d\,^2D_{5/2}$	2214.15	0.0032	0.0014	0.0000	0.0046
$4d\,^2D_{5/2} \rightarrow 5d\,^2D_{3/2}$	2222.84	0.0033	−0.0012	0.0000	0.0021
$5p\,^2P_{1/2} \rightarrow 5p\,^2P_{3/2}$		1.1545	0.0000	0.0000	1.1545
$4f\,^2F_{5/2} \rightarrow 4f\,^2F_{7/2}$		1.8516	0.0000	0.0000	1.8516
$5d\,^2D_{3/2} \rightarrow 5d\,^2D_{5/2}$		1.5492	0.0001	0.0000	1.5493

amplitudes vary between 1.5% and 7.5% leading to about 3% to 15% variations in the transition probabilities from the corresponding DF values [26]. Here also, the Gaunt contributions are found to be less than 0.1%, except for the $4p\,^2P_{3/2} \rightarrow 4f\,^2F_{5/2,7/2}$ (about 0.104%) and $4p\,^2P_{3/2} \rightarrow 5p\,^2P_{1/2}$ (about 0.116%) transitions.

The $M1$ transition amplitudes are presented in Table IV along with the correlation and Gaunt contributions. The transitions between the fine structure states have significant amplitudes with respect to the amplitudes of other transitions. The Gaunt contributions to all these fine structure transitions are seen to be zero. However, the correlation contributions to a few of these fine structure transitions are nonzero, but have very small values, as can be seen from Table IV. Therefore, the DF results of the $M1$ transitions between the fine structure states can provide excellent approximations of the totals. Some of the $4d\,^2D_{3/2,5/2} \rightarrow 5d\,^2D_{3/2,5/2}$ transitions having relatively very small magnitudes are seen to have high percentage correlations. The Gaunt effects are found to have some nonzero values in the $4p\,^2P_{1/2,3/2} \rightarrow 5p\,^2P_{1/2,3/2}$ transitions as presented in Table IV.

Table V presents the lifetimes calculated by the CC approach and their comparisons with the other theoretical calculations and experimental measurements. The lifetime of the $5s\,^2S_{1/2}$ state is calculated for the first time. Here, these calculations are performed using the transition amplitudes obtained by the CC theory and the experimental transition energies of the NIST [28]. One can find excellent agreement between the present calculations and the theoretical results obtained by the Coulomb-approximated Hartree-Slater core potential method [8]. Except for the $4d\,^2D_{3/2}$ state, our calculations agree well with the beam-foil measurements with an average discrepancy of 5.5% [12]. In the case of the $4d\,^2D_{3/2}$ state, the experimental uncertainty is considerably large and both the theoretical results differ by about 25% from the experimental result.

The hyperfine A and B constants of Ga III with mass number 71 are presented in Tables VI and VII, respectively, and those with mass number 69 are presented in Tables VIII and IX, respectively. Both of these types of constants are presented within an approximate theoretical uncertainty of around ±1.5% [32]. To calculate these constants, the corresponding correlations and Gaunt contributions along with the DF results are also presented in the same tables. For the isotope ^{71}Ga, the nuclear spin, magnetic dipole moment, and electric quadrupole moment are considered as 3/2, 2.5623 μ_N, and 0.106 barns, respectively, whereas the same parameters for ^{69}Ga are taken as 3/2, 2.0166 μ_N, and 0.168 barns, respectively [13]. The ground-state, i.e., the $4s\,^2S_{1/2}$ state, hyperfine splitting values of ^{71}Ga III and ^{69}Ga III are calculated to be 34.95 and 27.51 GHz, respectively, which fall in the microwave region of the electromagnetic spectrum. In terms of length scale, these splitting values are associated with 0.86- and 1.09-cm lines which may be considered as useful parameters to find the isotopic abundances of ^{71}Ga III and ^{69}Ga III, respectively, in different astronomical systems. One can easily compute the hyperfine splitting values of the different excited states from Eq. (2.8) by employing our calculated hyperfine constants. These splitting values can provide linewidth estimations of a

TABLE V. Lifetimes of a few low-lying states and their comparisons with the other results (in 10^{-9} s).

		Other	
State	Present	a	b
$4p\,^2P_{1/2}$	1.29	1.35	1.20 ± 0.20
$4p\,^2P_{3/2}$	1.19	1.24	1.22 ± 0.10
$5s\,^2S_{1/2}$	0.60		0.56 ± 0.04
$4d\,^2D_{3/2}$	0.43	0.44	0.35 ± 0.15
$4d\,^2D_{5/2}$	0.44	0.46	0.42 ± 0.08

[a]Reference [8]. Coulomb approximation technique with a Hartree-Slater core.

[b]Reference [12]. Experimental measurement.

TABLE VI. Hyperfine A constants of ^{71}Ga III with the correlation and Gaunt contributions (in MHz).

State	DF	Δ_{corr}	Δ_{Gaunt}	Total
$4s\,^2S_{1/2}$	14 370.76	3093.24	10.50	17 474.50
$4p\,^2P_{1/2}$	2674.06	618.52	1.17	3293.75
$4p\,^2P_{3/2}$	489.41	119.45	0.32	609.18
$4d\,^2D_{3/2}$	90.40	40.73	0.31	131.44
$4d\,^2D_{5/2}$	38.68	18.23	0.12	57.03
$5s\,^2S_{1/2}$	3925.37	634.30	3.44	4563.11
$5p\,^2P_{1/2}$	875.59	158.32	0.59	1034.50
$5p\,^2P_{3/2}$	161.54	33.86	0.15	195.55

TABLE VII. Hyperfine B constants of ^{71}Ga III with the correlation and Gaunt contributions (in MHz).

State	DF	Δ_{corr}	Δ_{Gaunt}	Total
$4p\ ^2P_{3/2}$	56.864	20.130	−0.223	76.771
$4d\ ^2D_{3/2}$	3.489	3.845	−0.008	7.326
$4d\ ^2D_{5/2}$	4.936	5.424	−0.012	10.348
$5p\ ^2P_{3/2}$	18.770	5.158	−0.062	23.866

few transition lines in the visible and ultraviolet regions due to the hyperfine effects, which may be useful for obtaining a more accurate picture of abundance estimations in astrophysical systems like the HgMn stars [6].

As seen in Tables VI–IX, the hyperfine constants are highly correlated, but are affected comparatively little by the Gaunt interactions. The hyperfine A constants of the $4s\ ^2S_{1/2}$, $5s\ ^2S_{1/2}$, $4p\ ^2P_{1/2,3/2}$, and $5p\ ^2P_{1/2,3/2}$ states are about 16%–24% correlated, whereas those of the $4d\ ^2D_{3/2,5/2}$ states are about 45%–47% correlated. In the case of the B constants also, relatively strong correlations occur for the $4d\ ^2D_{3/2,5/2}$ states (about 110%) with respect to the $4p\ ^2P_{3/2}$ and $5p\ ^2P_{3/2}$ states (about 27%–35%). Due to such very high correlations, the hyperfine B constants of the $4d\ ^2D_{3/2,5/2}$ states at the CC levels become more than two times the corresponding DF values. For the $4s\ ^2S_{1/2}$, $5s\ ^2S_{1/2}$, $4p\ ^2P_{1/2,3/2}$, and $5p\ ^2P_{1/2,3/2}$ states, the Gaunt contributions to the A constants are less than 0.1%, but for the $4d\ ^2D_{3/2,5/2}$ states, these are about 0.21%–0.24%. Contrary to the A constants, the Gaunt contributions to the B constants of the $4d\ ^2D_{3/2,5/2}$ states (about 0.11%) are found to be less compared to those of the $4p\ ^2P_{3/2}$ and $5p\ ^2P_{3/2}$ states (about 0.26%–0.29%). Moreover, these contributions arise with opposite signs between both these types of constants for all the concerned states.

An interesting consequence of the self-consistent treatments of the Gaunt interaction at the DF and CC levels of the hyperfine A and B constants can be observed in Fig. 1. Here, percentage change of the Gaunt contribution due to the correlation effect is defined by $\{[(\Delta_{Gaunt}) - (\Delta_{Gaunt})_{DF}]/[|(\Delta_{Gaunt})_{DF}|]\} \times 100\%$, where $(\Delta_{Gaunt})_{DF}$ is the Gaunt contribution at the DF level [15]. This plot shows dramatic changes in the Gaunt contributions due to the correlation effects in the A constants of all the states. Especially in the A constants of the $4d\ ^2D_{3/2,5/2}$ states, these changes are about 575%–650%. However, in the B constants, these changes are about 30%–35% for the $4p\ ^2P_{3/2}$ and $5p\ ^2P_{3/2}$ states, but are about 150%–225% for the $4d\ ^2D_{3/2,5/2}$ states. In this figure, one can also see opposite trends of this feature between these two types of constants. It has been observed that the Gaunt contributions are negative for both these types of constants at the DF levels of all the states. But due to the correlation effects, these contributions are seen to move from negative to positive values for the A constants and become negative to more negative for the B constants.

TABLE VIII. Hyperfine A constants of ^{69}Ga III with the correlation and Gaunt contributions (in MHz).

State	DF	Δ_{corr}	Δ_{Gaunt}	Total
$4s\ ^2S_{1/2}$	11 310.76	2434.59	8.26	13 753.61
$4p\ ^2P_{1/2}$	2104.56	486.79	0.93	2592.28
$4p\ ^2P_{3/2}$	385.18	94.01	0.25	479.44
$4d\ ^2D_{3/2}$	71.15	32.05	0.25	103.45
$4d\ ^2D_{5/2}$	30.44	14.35	0.10	44.89
$5s\ ^2S_{1/2}$	3089.53	499.24	2.71	3591.48
$5p\ ^2P_{1/2}$	689.12	124.60	0.46	814.18
$5p\ ^2P_{3/2}$	127.13	26.66	0.12	153.91

TABLE IX. Hyperfine B constants of ^{69}Ga III with the correlation and Gaunt contributions (in MHz).

State	DF	Δ_{corr}	Δ_{Gaunt}	Total
$4p\ ^2P_{3/2}$	90.125	31.905	−0.354	121.676
$4d\ ^2D_{3/2}$	5.530	6.093	−0.013	11.610
$4d\ ^2D_{5/2}$	7.823	8.596	−0.019	16.400
$5p\ ^2P_{3/2}$	29.749	8.174	−0.098	37.825

IV. CONCLUSION

The $E1$, $E2$, and $M1$ transition amplitudes of Ga III have been calculated employing a highly correlated method with a relativistic correction. The lifetimes of some low-lying states have been estimated from these calculations. The contributions from the electron correlations and Gaunt interactions to these transition amplitudes have been discussed in detail. Investigation of the ground-state hyperfine splitting of both the isotopes considered here predicts their possible use as frequency standards at a fraction of a nanosecond. The calculated hyperfine constants for some low-lying states of these isotopes may be considered as important parameters for abundance analysis in some visible and ultraviolet lines from different astronomical objects. The correlation effects on the Gaunt contributions to the hyperfine A and B constants have been found to have opposite trends. We hope, our spectroscopic study may in the future help the astrophysicists regarding the issue of the Gallium Problem in HgMn stars.

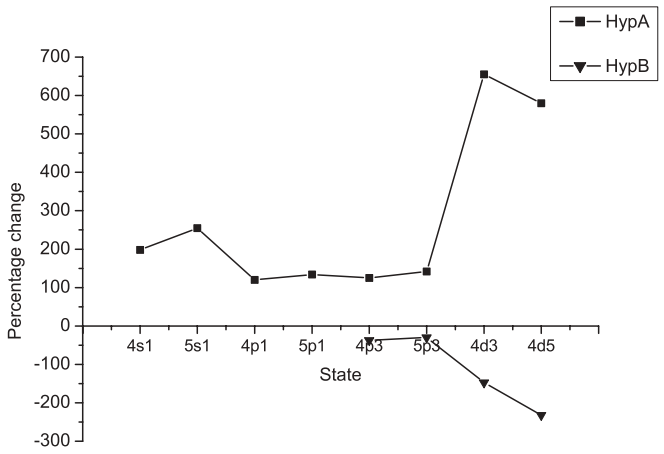

FIG. 1. Percentage changes of the Gaunt contributions due to the correlation effects in the hyperfine A (HypA) and B (HypB) constants of $4s\ ^2S_{1/2}$ (4s1), $5s\ ^2S_{1/2}$ (5s1), $4p\ ^2P_{1/2}$ (4p1), $5p\ ^2P_{1/2}$ (5p1), $4p\ ^2P_{3/2}$ (4p3), $5p\ ^2P_{3/2}$ (5p3), $4d\ ^2D_{3/2}$ (4d3), and $4d\ ^2D_{5/2}$ (4d5) states.

ACKNOWLEDGMENTS

We are very much grateful to Professor B. P. Das and Dr. R. K. Chaudhuri, Indian Institute of Astrophysics, Bangalore, India, and Dr. B. K. Sahoo, Physical Research Laboratory, Ahmedabad, India, for providing the CC code in which we implemented the Gaunt interaction part. The calculations were carried out by the servers of IIT Kharagpur, India. We would like to recognize help from the Council of Scientific and Industrial Research (CSIR), India, and the Board of Research in Nuclear Sciences (BRNS), India, for funding.

[1] M. M. Schauer, J. R. Danielson, D. Feldbaum, M. S. Rahaman, L.-B. Wang, J. Zhang, X. Zhao, and J. R. Torgerson, Phys. Rev. A **82**, 062518 (2010).
[2] V. A. Dzuba, V. V. Flambaum, and M. V. Marchenko, Phys. Rev. A **68**, 022506 (2003).
[3] C. J. Campbell, A. V. Steele, L. R. Churchill, M. V. DePalatis, D. E. Naylor, D. N. Matsukevich, A. Kuzmich, and M. S. Chapman, Phys. Rev. Lett. **102**, 233004 (2009).
[4] S. J. O'Toole, Astron. Astrophys. **423**, L25 (2004).
[5] M. Takada-Hidai, K. Sadakane, and J. Jugaku, Astrophys. J. **304**, 425 (1986).
[6] M. M. Dworetsky, C. M. Jomaron, and Claire A. Smith, Astron. Astrophys. **333**, 665 (1998).
[7] K. E. Nielsen, G. M. Wahlgren, C. R. Proffitt, D. S. Leckrone, and S. J. Adelman, Astron. J. **130**, 2312 (2005).
[8] L. J. Curtis and C. E. Theodosiou, Phys. Rev. A **39**, 605 (1989).
[9] J. Migdalek and W. E. Baylis, J. Phys. B **12**, 1113 (1979).
[10] Hsiang-Shun Chou and W. R. Johnson, Phys. Rev. A **56**, 2424 (1997).
[11] L. C. Owono Owono, M. G. Kwato Njock, and M. L. C. Owono Angue, Phys. Lett. A **339**, 343 (2005).
[12] W. Ansbacher, E. H. Pinnington, J. L. Bahr, and J. A. Kernahan, Can. J. Phys. **63**, 1330 (1985).
[13] P. Raghavan, At. Data Nucl. Data Tables **42**, 189 (1989).
[14] J. A. Gaunt, Proc. R. Soc. London, Ser. A **122**, 513 (1929).
[15] N. N. Dutta and S. Majumder, Phys. Rev. A **85**, 032512 (2012).
[16] J. B. Mann and W. R. Johnson, Phys. Rev. A **4**, 41 (1971).
[17] G. Dixit, B. K. Sahoo, R. K. Chaudhuri, and S. Majumder, Phys. Rev. A **76**, 042505 (2007).
[18] I. Lindgren and J. Morrison, *Atomic Many-body Theory*, edited by G. Ecker, P. Lambropoulos, and H. Walther (Springer, Berlin, 1985), Vol. 3.
[19] I. Lindgren and D. Mukherjee, Phys. Rep. **151**, 93 (1987).
[20] S. Pal, M. Rittby, R. J. Barlett, D. Sinha, and D. Mukherjee, Chem. Phys. Lett. **137**, 273 (1987); J. Chem. Phys. **88**, 4357 (1988).
[21] B. K. Sahoo, R. K. Chaudhuri, B. P. Das, H. Merlitz, and D. Mukherjee, Phys. Rev. A **72**, 032507 (2005).
[22] W. R. Johnson, D. R. Plante, and J. Sapirstein, Adv. At. Mol. Opt. Phys. **35**, 255 (1995).
[23] H. S. Nataraj, B. K. Sahoo, B. P. Das, R. K. Chaudhuri, and D. Mukherjee, J. Phys. B **40**, 3153 (2007).
[24] K. T. Cheng and W. J. Childs, Phys. Rev. A **31**, 2775 (1985).
[25] G. Dixit, H. S. Nataraj, B. K. Sahoo, R. K. Chaudhuri, and S. Majumder, Phys. Rev. A **77**, 012718 (2008).
[26] N. N. Dutta and S. Majumder, Astrophys. J. **737**, 25 (2011).
[27] F. A. Parpia, C. F. Fischer, and I. P. Grant, Comput. Phys. Commun. **175**, 745 (2006).
[28] A. Kramida, Yu. Ralchenko, J. Reader, and NIST ASD Team (2012). *NIST Atomic Spectra Database* (ver. 5.0) [Online]. Available at http://physics.nist.gov/asd [2012, August 1]. National Institute of Standards and Technology, Gaithersburg, MD.
[29] J. Migdalek, J. Quant. Spectrosc. Radiat. Transfer **20**, 81 (1978).
[30] S. Hameed, A. Herzenberg, and M. J. James, J. Phys. B **1**, 822 (1968).
[31] Jon C. Weisheit, Phys. Rev. A **5**, 1621 (1972).
[32] The Editors, Phys. Rev. A **83**, 040001 (2011).